
# Sticking particles to solid surfaces using Moringa oleifera proteins as a glue



Citation for the original published paper (version of record):
Nouhi, S., Pascual, M., Hellsing, M. et al (2018). Sticking particles to solid surfaces using Moringa oleifera proteins as a glue. Colloids and Surfaces B: Biointerfaces, 168: 68-75.
http://dx.doi.org/10.1016/j.colsurfb.2018.01.004

Colloids and Surfaces B: Biointerfaces 168 (2018) 68–75

Contents lists available at ScienceDirect

Colloids and Surfaces B: Biointerfaces

journal homepage: www.elsevier.com/locate/colsurfb

# Sticking particles to solid surfaces using *Moringa oleifera* proteins as a glue☆

Shirin Nouhi[a], Marc Pascual[a,1], Maja S. Hellsing[a], Habauka M. Kwaambwa[b], Maximilian W.A. Skoda[c], Fredrik Höök[d], Adrian R. Rennie[a,*]

[a] Centre for Neutron Scattering, Uppsala University, Box 516, 751 20, Uppsala, Sweden
[b] Namibia University of Science and Technology, Faculty of Health and Applied Sciences, Private Bag 13388, 13 Storch Street, Windhoek, Namibia
[c] Rutherford Appleton Laboratory, Harwell, Didcot OX11 0QX, United Kingdom
[d] Department of Applied Physics, Chalmers University of Technology, Gothenburg, Sweden

ARTICLE INFO

*Article history:*
Received 25 September 2017
Received in revised form 5 December 2017
Accepted 6 January 2018
Available online 8 January 2018

*Keywords:*
Latex particles
Moringa oleifera
Surface scattering
Adhesion
Quartz

ABSTRACT

Experimental studies have been made to test the idea that seed proteins from *Moringa oleifera* which are novel, natural flocculating agents for many particles could be used to promote adhesion at planar interfaces and hence provide routes to useful nanostructures. The proteins bind irreversibly to silica interfaces. Surfaces that had been exposed to protein solutions and rinsed were then exposed to dispersions of sulfonated polystyrene latex. Atomic force microscopy was used to count particle density and identified that the sticking probability was close to 1. Measurements with a quartz crystal microbalance confirmed the adhesion and indicated that repeated exposures to solutions of *Moringa* seed protein and particles increased the coverage. Neutron reflectivity and scattering experiments indicate that particles bind as a monolayer. The various results show that the 2S albumin seed protein can be used to fix particles at interfaces and suggest routes for future developments in making active filters or improved interfaces for photonic devices.



## 1. Introduction

Proteins from *Moringa* seeds have attracted wide scientific attention in recent years largely because of their potential applications rather than seeking to understand the biological role. There are 14 species of *Moringa* [1,2] and some are widely cultivated, in particular, *Moringa oleifera*, although native to the Indian subcontinent is exploited for its leaves, oil and as a source of food [3]. A particular interest has been the exploitation of crushed seeds for water purification that has been known traditionally for many years but attracted scientific studies since the 1980′s [4–6].

The *Moringa* seed proteins have been identified as effective flocculating agents for a wide range of impurities (see e.g. [7]). They can replace the usual industrial produced materials that are normally either cationic polymers [8] or polyvalent salts. Major advantages for the use of *Moringa* seeds in this application arise from its low toxicity and negligible environmental impact. This allows water treatment processes to be developed that can be used on a domestic or village scale in remote areas without trained technical supervision. In many countries with major needs for such technologies, the *Moringa* trees can be grown readily even under conditions of low rainfall.

Some more recent studies have focused on understanding the details of interactions of the protein molecules with various surfaces and with other molecules [9–14]. Although these may be dominated by the overall net positive charge at neutral pH, there are strong indications that self-association of the proteins is important and that adsorption occurs at a range of interfaces [11,14]. These interactions strongly encourage flocculation and heteroflocculation of a wide range of materials. At some surfaces, such as alumina, displacement of the protein by rinsing with a cationic surfactant was observed [14].

It is now established that a major component of the proteins is a 2S albumin. A crystal structure has been established [15] but the behaviour of this protein is not identical to the mixture found in the crude extract as it has been found not to adsorb to alumina interfaces at neutral pH [16]. Understanding the details of

☆ This article has been prepared to mark the 65th birthday of Professor Piero Baglioni. Many of the authors have enjoyed scientific discussions with Piero and benefited from his enthusiasm for solving interdisciplinary practical challenges by application of fundamental principles of colloid and surface science.

* Corresponding author.
*E-mail address:* adrian.rennie@physics.uu.se (A.R. Rennie).
[1] Present address: UMR CNRS Gulliver 7083, ESPCI ParisTech, 10 rue Vauquelin, F-75005 Paris, France.

https://doi.org/10.1016/j.colsurfb.2018.01.004

the interactions offers the prospect of designing materials that could separate specific types of particles dispersed in water, either alone or when combined with specific other surfactants. The use of sand that has been prepared with pre-coated layers of *Moringa* protein as antimicrobial filters has been suggested by Jerri et al. [17]. However, the specific range of direct antimicrobial activity and its mechanism is still the subject of ongoing studies. It is known from a number of studies that the proteins extracted from seeds can vary according to the conditions of sample preparation. Some explicit descriptions of various materials with different molecular mass have been described previously [18–20]. As practical applications of seed products, such as for water purification, would use a crude extract, most studies have been conducted with samples that contain a range of proteins.

Binding particles at interfaces can be of a great importance not only in respect of filters but also to retain self-assembled structures that may be formed at interfaces. For example, colloidal particles have been shown to form large domains of crystalline structure at solid/liquid interfaces [21] which can be used directly for low-cost technique manufacture of photonic devices [22]. However, it is common that the formed structures crack and particles tend to move during the drying process. For such applications, it is also valuable to develop means to fix defined nanostructures in place.

The present study uses a range of techniques to investigate the use of an extract of *Moringa* protein that is pre-adsorbed on silica surfaces as a means to bind particles in a controlled manner at interfaces. Experiments have been made to explore the binding of polystyrene latex particles, of two sizes, with a small negative charge to silica surfaces at which they would not normally attach.

## 2. Methods and materials

### 2.1. Apparatus

Atomic force microscopy, AFM, uses a physical tip attached to a flexible cantilever to move across the surface of the sample and provide topography images at the nanometre scale [23–25]. In this study, the tapping mode of AFM was used on dried samples. This method did not provide images of the substrate/protein interface but was used primarily to investigate the number of particles that are stuck to the surface and compare the distribution of the particles in the presence and absence of a pre-adsorbed protein layer in different particle/protein concentrations. A Nanosurf Mobile-S with 190 Al-G tips was used and most images were 5 mm × 5 μm with 256 lines scanned.

A quartz crystal microbalance (QCM) consists of a quartz crystal which is oscillated at its resonant frequency in a shear mode. If mass is added or removed from the crystal, a frequency shift, $\Delta f$ is observed which according to the Sauerbrey [26,27] law is linearly related to the changes in mass, $\Delta m$, as:

$$\Delta f = -C_f \Delta m \quad (1)$$

where $C_f$ is a constant that depends only on the sensitivity of the crystal.

Quartz crystal microbalance with dissipation monitoring (QCM-D) provides a simultaneous measurement of changes in the dissipation factor, $D$, as well as the oscillation frequency of the crystal at the fundamental frequency and higher overtones. The dissipation is the ratio of the energy lost per cycle to that of the elastic energy and is determined from the decay of amplitude after excitation [28]. A Q-Sense E4 instrument was used. Information contained in combined $\Delta f$ and $\Delta D$ measurements at multiple overtones was used, which for rigid nanoparticles has been previously shown to offer information about film thickness [29].

Neutron reflectometry was used to quantify, in-situ, the adsorption of proteins to the surface and binding of particles to the protein layer. Neutrons interact with the nuclei of atoms and this allows them to penetrate deep into the sample with few interactions. The high penetration depth of neutrons makes some materials such as silicon to be so-called transparent for neutrons. This is an advantage of neutrons over, for example, AFM technique since one can probe the structure at the solid-liquid interfaces by illuminating the interface from the solid side. The neutron reflectivity experiment was performed on the reflectometer INTER at the ISIS facility, Rutherford Appleton Laboratory, UK [30] with a reflecting sample surface that is close to horizontal. The time-of-flight mode uses wavelengths from 2 to 14 Å to provide data in a momentum transfer, $Q$, range between 0.01 and 0.34 $Å^{-1}$, however, the samples in this study showed measurable signal up to about 0.12 $Å^{-1}$. The collimation slits and the data collection were chosen to provide resolution in momentum transfer, $\Delta Q/Q$, of about 2.5 percent. Specular reflectivity was measured using a point detector at 0.5 and 2.3°. Off-specular scattering data were measured with a linear detector at each angle to record the scattering above and below the reflected beam as a function of neutron wavelength.

The sample holder has been described previously [31]. The solution was sealed with a PTFE gasket between the quartz crystal and a polycarbonate base with injection and outlet ports. The base contains a small stirring magnet to keep the samples spread uniformly within the cell. The temperature was maintained at 25 °C during the measurements using a Julabo bath that circulated water through the metal parts that clamp the crystal and the base.

### 2.2. Interpretation of neutron reflection data

In this experiment, neutron reflection was used in both specular ($\theta_i = \theta_f$) and off-specular ($\theta_i \neq \theta_f$) conditions, where $\theta_i$ is the angle of the incident beam and $\theta_f$ is the angle of the outgoing beam, in order to investigate the out-of-plane and in-plane structure of particles stuck to the surface. Neutron reflectivity, R($Q$), is defined as the ratio between the intensity of the reflected beam over the intensity of the incident beam, at the specular condition. Reflectivity in the specular condition, where $Q$ is perpendicular to the interface, is commonly shown as a function of magnitude of momentum transfer, $Q$, and it provides information such as the thickness, composition, and roughness of layers parallel to the interface. The momentum transfer perpendicular to the interface is given by:

$$Q = (4\pi/\lambda)\sin(\theta_i) \quad (2)$$

where λ is the wavelength of the neutrons and $\theta_i$ is the grazing angle of incidence. Reflectivity is calculated using the characteristic optical matrix of the stratified layers which is defined by scattering length density, ρ:

$$\rho = \Sigma n_i b_i \quad (3)$$

where $n_i$ is the number density for atoms of element, i, $b_i$ is the scattering length and the sum is taken over all of the elements found in a layer. Different isotopes have different scattering lengths for neutrons and this allows one to increase the contrast and choose the scattering interface, by carefully choosing the dispersion phase. For example, it is convenient to study the adsorption of *Moringa* proteins or polystyrene particles in $D_2O$ rather than $H_2O$ (see Table 1 for the values of scattering length density). The total scattering length density, ρ, of each layer is given as:

$$\rho = \rho_w \varphi_w + \rho_d \varphi_d \quad (4)$$

where $\rho_w$ and $\varphi_w$ are the scattering length density and volume fraction of water, and $\rho_d$ and $\varphi_d$ are those of the dissolved or dispersed material.

**Table 1**
Materials Used in the Study; Neutron Scattering Lengths and Scattering Length Densities.

| Name | Formula | Formula Mass/g mol$^{-1}$ | Density /g cm$^{-3}$ | Molecular volume /Å$^3$ | Scattering length** Σ b /fm | ρ /10$^{-6}$ Å$^{-2}$ |
|---|---|---|---|---|---|---|
| Water | $H_2O$ | 18 | 0.9975 | 30 | −1.7 | −0.56 |
| Heavy water | $D_2O$ | 20 | 1.105 | 30 | 19.1 | 6.35 |
| Quartz | $SiO_2$ | 60.08 | 2.66 | 37.6 | 15.8 | 4.12 |
| *Moringa* protein in $H_2O$* | | 9900 | 1.35 | 12400 | 1770 | 1.46 |
| *Moringa* protein in $D_2O$* | | 10000 | 1.36 | 12400 | 3150 | 2.60 |
| Polystyrene | $C_8H_8$ | 104.15 | 1.05 | 164.7 | 23.24 | 1.41 |
| Hexadecyltrimethylammonium bromide | $C_{16}H_{33}N(CH_3)_3Br$ | 364.45 | 1.14 | 530.9 | −14.67 | −0.35 |

*The density for the protein was determined by Maikokera [32]. The molecular mass of the proteins is taken from the study of Moulin et al. [16]. **The scattering lengths were taken from Sears [33].

Neutron reflectivity data for the interfaces were modelled using the programs available on the web [34] that are designed to fit specific, physically realistic models appropriate to the systems being investigated. The program *cprof* was used to model data with a diffuse layer of protein at the interface and *ferje* to fit density profiles that correspond to layers of spherical particles. The effects of instrument resolution and background scattering were included in the fits.

Off-specular scattering was measured for some of the samples in order to investigate whether there is any structural information in other directions rather than perpendicular to the interface, for example, in-plane correlation between particles.

### 2.3. Materials

#### 2.3.1. Moringa *proteins*

The *Moringa oleifera* seeds were obtained from suppliers in Botswana and Zambia and the protein powder was extracted using the experimental method described previously by Kwaambwa and Maikokera [9–11]. The proteins that were found in the extract used in the present experiments have been separated and identified using chromatography and mass spectrometry [16]. The main protein species were between 11.8 and 12.0 kDa. The zeta potential of the protein extract in aqueous solution at neutral pH was found to be 14 ± 2 mV [12]. The isoelectric point is around pH 10–11 and this is well above the neutral pH used in the current study.

The stock solution of protein was made in $D_2O$ with a concentration of 0.1 wt.% for the neutron experiments and at 0.2 wt.% in $H_2O$ for AFM and QCM-D measurements. The sample was tumbled for a few hours and was injected in the sample cell at the desired concentration using an HPLC pump for the neutron measurements and a peristaltic pump for the QCM-D experiments.

#### 2.3.2. Colloidal particles and Solid Surfaces

Charge stabilized polystyrene latex particles were synthesized and characterized as described in previous articles [35,36]. Two sizes of particles with 720 Å radius, polydispersity <1%, designated PS3 and particles of radius 350 Å, polydispersity <5%, designated PS11 were used in the various experiments. The surface potential of the particles was determined using a Malvern Zetasizer nano to be about −30 mV for the PS3 latex and −35 mV for the PS11 at pH 7. The various physical parameters for the materials used in this study and needed in analysis of neutron data are shown in Table 1.

Substrates used for the neutron experiments were single crystals of quartz, $SiO_2$, 5 cm × 5 cm × 1 cm with a Z-cut on the large face supplied by Crystran Ltd., Poole, U.K. The crystals were cleaned prior to the experiment following the cleaning procedure described previously [37]. Briefly, the crystals were first immersed in diluted Decon90 in a clean Petri dish for a few minutes and then rinsed with pure water. Drops of concentrated sulfuric acid were then spread over the reflecting surface of the crystal, followed by approximately the same amount of water and after a few minutes, the surface was rinsed extensively with water. Cleaning with acid was repeated up to three times until the surface of crystal became completely hydrophilic. Two quartz crystals were used for the experiment, and both were characterised at the start of the experiment with neutrons using $D_2O$, $H_2O$ and a mixture of 68:32 $D_2O$:$H_2O$ that matches the scattering length density of the quartz. The data and model fits are presented in Fig. S1 in the supporting information. Neutron reflection results showed that both crystals were nearly identical with a roughness <10 Å. Surfaces used for AFM measurements were borosilicate glass microscope cover slips that were cleaned in the same way as the crystal substrates used for neutron experiments. The surfaces used for the QCM-D experiment were silica and were cleaned first with detergent solution and water. Subsequently, before the experiment, they were cleaned twice using a UV-ozone treatment followed by extensive rinsing with water. The roughness of surfaces used for QCM-D measurements were indicated by the supplier to be less than <10 Å [38] that is about the same as that of the quartz crystals used for neutron experiments.

### 2.4. Experimental procedures

Different techniques were used in this study to compare behaviour and also to determine the various interactions that govern binding of particles and *Moringa oleifera* proteins at solid-liquid interfaces. QCM-D was used initially to determine whether particles and proteins bind together at the interface. The scattering reflection experiments investigated conditions similar to those used in QCM-D but in longer equilibrium time. Neutron reflection could provide in-situ, average structural information over time scales of one to a few hours for each sample compared to QCM-D measurements where the measurement times were some minutes although samples could be equilibrated for longer. QCM-D and reflection experiments both provide in-situ structural information, however, the neutron scattering experiment was limited by the availability of the instrument time. AFM was used to determine the adhesion by counting particles after samples were rinsed and dried. The samples were prepared with low concentrations of particles so that multilayers were not formed and this allowed more accurate estimates of the number density of particles from the images to be made. The neutron scattering and QCM-D experiments were performed with higher concentrations of particles to explore faster equilibration.

## 3. Results and discussion

Fig. 1 shows neutron reflectivity from the adsorbed layer of *Moringa* proteins to the quartz surface at different concentrations of protein solution. The adsorption could be described with two layers of uniform densities adsorbed to the quartz and a further layer with an exponential decay as seen previously at other surfaces [11,14]. After exposure of the surface to the highest concentration of protein, 0.1 wt.%, it was rinsed with water and characterised using two contrasts of water ($D_2O$ and $H_2O$). Simultaneous fits to both data sets showed a protein layer near the surface that was 32 Å thick

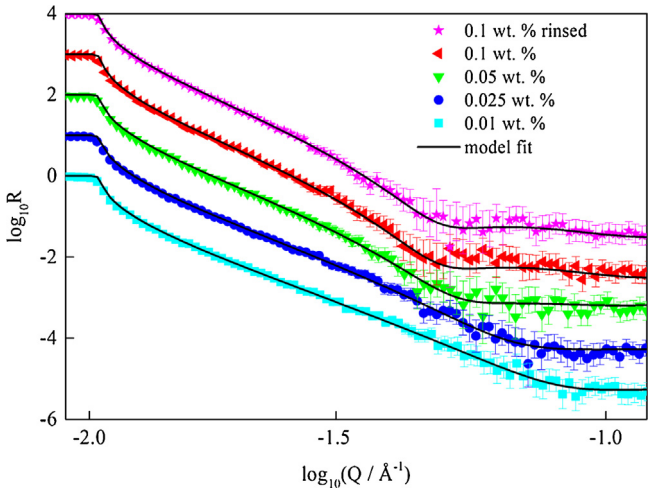


**Fig. 1.** Neutron reflectivity data for *Moringa oleifera* proteins adsorbed onto the quartz surface from solutions with different concentration in $D_2O$. The notable similarity of the sample rinsed with $D_2O$ to that for the 0.1 wt.% solution indicates that the protein is not removed from the surface with water. Each curve is offset by an order of magnitude for clarity.

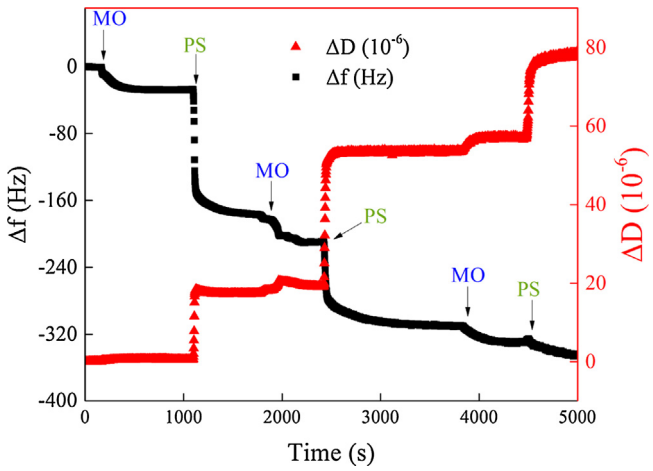


**Fig. 3.** QCM-D data for an experiment with repeated sequential injection of 1 mg mL$^{-1}$ of *Moringa oleifera* protein, labelled MO and 0.5 wt.% small (PS11) particles, labelled PS. The sample was rinsed with water after each injection. The frequency shift is shown on the left axis (squares) and changes in the dissipation on the right axis (triangles).

with scattering length density of $4.7 \times 10^{-6}$ Å$^{-2}$ in $D_2O$ which corresponds to a layer containing about 47 % protein, with a further lower density layer and then an exponential decay towards the bulk solution. The adsorbed layer observed at different concentrations as shown in Table S1 of the supporting information, were very similar to those found in a previous study [11] of binding to an amorphous silica layer on a silicon crystal. These are consistent with formation of multilayers of protein. Such extended structures that contain a lot of water might arise as a consequence of the extracted sample containing a mixture of different proteins possibly favoured by specific co-adsorption.

The amount of protein adsorbed to the surface at each concentration calculated from the model fits is shown in Fig. 2. The adsorption of the proteins in the same concentration range was also measured using a QCM-D. These data could be fitted using a conventional Kelvin-Voigt viscoelastic model [39]. The thickness

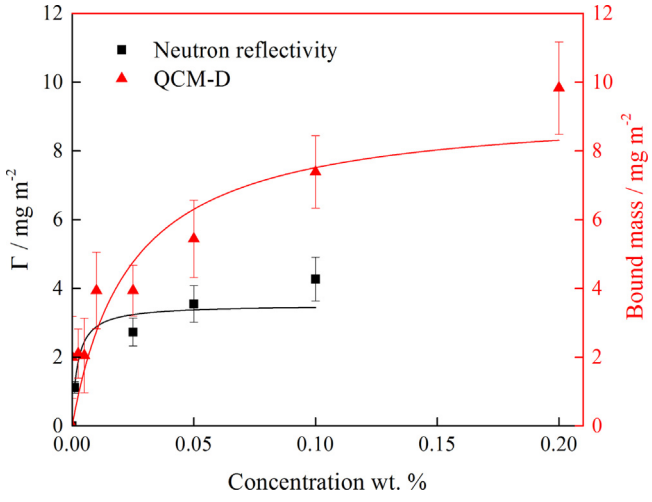


**Fig. 2.** Surface excess, Γ, of the proteins at the quartz/solution interface for different concentrations. Results are taken from the fits to the neutron reflection data shown in Fig. 1. The results can be compared with the bound mass observed in QCM-D experiments (data and fitting parameters are shown in supporting information) which corresponds to the amount of protein together with the water with which it is tightly associated and is consequently more than the surface excess of the protein determined by neutron reflection. The solid lines are fits to the Langmuir adsorption isotherm for each data set.

and density of the fitted layer at each concentration are shown in Table S2 and Fig. S3. However, the results indicate that a lot of water is trapped in the layer, as seen with neutron reflectivity. The mass attached to the interface is therefore overestimated using QCM-D technique compared to neutron reflectivity. The difference is evident from Fig. 2.

We have shown previously that charge stabilized polystyrene colloidal particles can self-assemble into crystalline structures close to a solid surface. QCM-D, AFM and neutron reflectivity showed that the latex particles on their own, do not stick to the surface and are completely removed when the surface is rinsed. QCM-D studies with the particles alone on a clean surface without protein showed a positive frequency shift when the mass was added to the layer which did not follow the Sauerbrey relation (equation 1) for a rigid layer adsorbed to the surface. The data could only be modelled with a water gap between the particles and the solid surface [40]. The present results show clearly that when the particles are exposed to a surface with a pre-adsorbed layer of protein, QCM-D data have the expected responses, i.e. decrease in frequency and increase in dissipation with added material, indicating the adsorption of firmly interacting components. Fig. 3 shows QCM-D data from sequential injections of 1 mg mL$^{-1}$ *Moringa oleifera* protein and 0.5 wt.% polystyrene particles (PS11) with continuous rinsing of water in-between.

Similar behaviour was observed using AFM and neutron reflectivity. Neutron reflectivity data from the particles on their own at the quartz-water interface is shown in Fig. 4a. Data showed the critical angle at 0.01 Å$^{-1}$, as expected for a quartz/$D_2O$ interface. The reflectivity was similar to that of the bare surface and could be modelled with the same parameters as the bare surface indicating that there was no significant adhered layer. In contrast, the reflectivity data from the particles in the presence of protein layer, even after the rinsing, showed clear fringes corresponding to the adsorption of a layer of latex. Fig. 4a shows reflectivity data from 0.5 wt.% PS3 particles on the quartz surface in the presence of adsorbed protein layer. The model used for fitting reflectivity data from particles and proteins accounts for the reflectivity from spherical particles adsorbed on the pre-characterised layer of protein. The model slices the layer/layers of particles into planes parallel to the surface. In each layer, depending on the coverage of particles and distance from the centre of particles, a certain fraction is occupied by the particles and the rest is filled with water. The inset plot at the top right of Fig. 4a shows the scattering length density profile for the

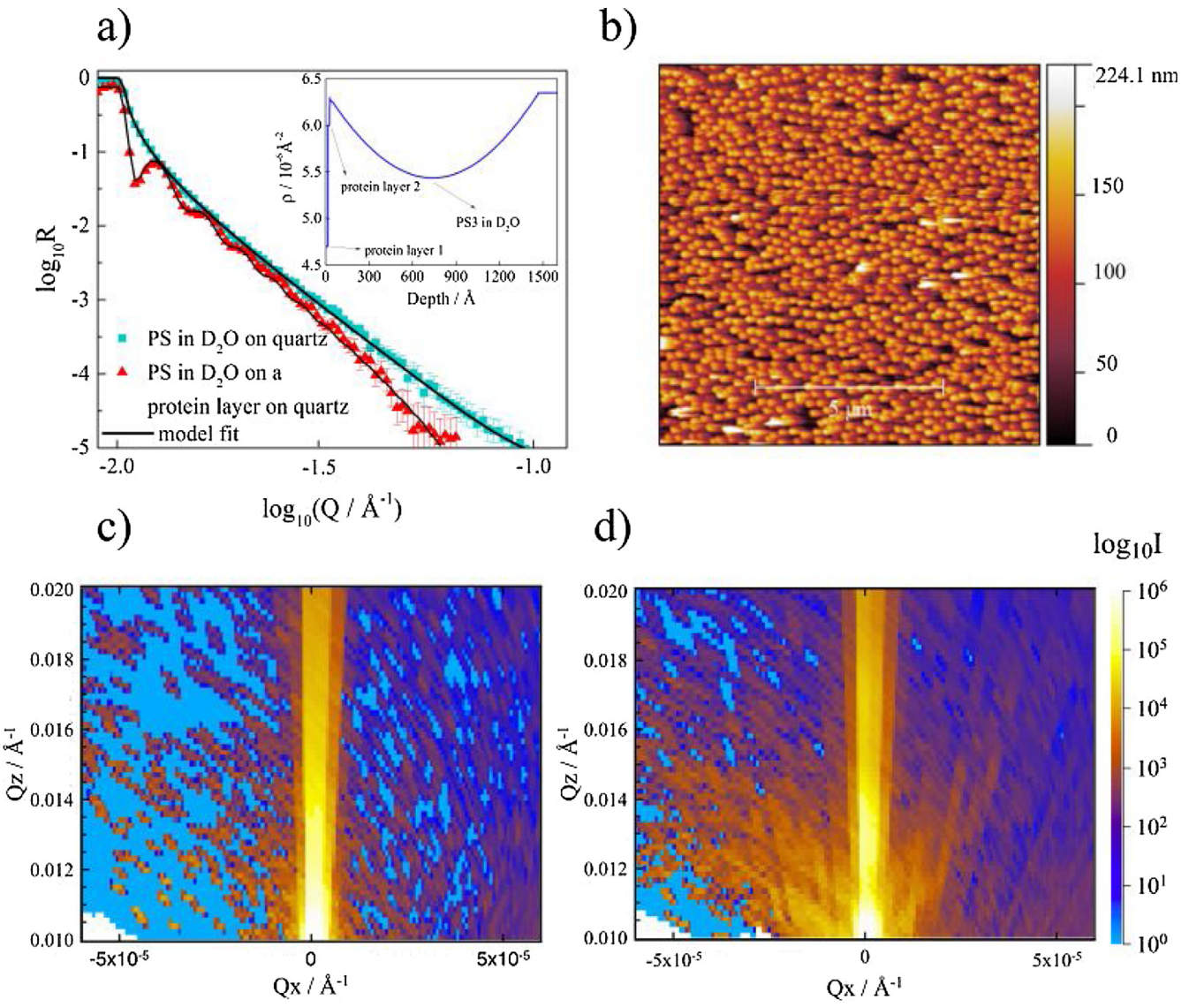


**Fig. 4.** (a) Specular reflectivity data and model fit showing the adsorption of particles to the quartz surface in the presence of a pre-adsorbed protein layer compared to the reflection from the particles against bare quartz surface. Scattering length density profile of the structure calculated by the model is shown on the top right. (b) AFM image of the same surface measured after the experiment. The surface was dried after rinsing and showed areas with high particle density and order. (c) Two-dimensional scattering map of the surface with *Moringa oleifera* protein adsorbed from 0.1 wt.% solution on the quartz surface before injection of the particle dispersion and (d) after injecting the PS3 particles and rinsing with water. Scattering along $Q_x = 0$ corresponds to the specular reflection. Diffuse scattering as described by Yoneda [41] appears in the presence of particles on the surface and arises from roughness in the interfacial structure.

PS3 particles adsorbed to the protein layer that was calculated as the model in the fit.

The model fit showed that a monolayer of particles was formed with a fractional coverage of approximately 17 %. Similar results were seen for small (PS11) particles with a slightly lower coverage (about 13 %), the data, model fits and density profile for these particles are shown in Fig. S4 in the supporting information. Particles at the surface were not removed by extensive rinsing with either water or a 2 mmol $L^{-1}$ solution of the cationic surfactant hexadecyltrimethylammonium bromide ($C_{16}$TAB). Two-dimensional scattering map, shown in Fig. 4c and d, indicates a diffuse signal in off-specular region, so-called Yoneda [41] scattering that appears when particles stick to the protein. This scattering arises from non-uniformity or interfacial roughness in the structure. An alternative representation of the same data as wavelength-angle maps of intensity is provided in the supporting information, Fig. S5 where some geometrical and wavelength effects are more clearly seen. After the neutron experiment, the substrates were rinsed, dried and then scanned with AFM. The image in Fig. 4b showed that the particles have formed some regions that are closely packed and thus the layer has to be non-uniform. Clustering that is observed on drying suggests that particles although bound to the surface can have lateral mobility.

The number of particles attached to the surface was observed to vary with the concentration of particles as well as the deposition time. In order to estimate the sticking probability of particles, systematic measurements were performed at low concentrations of particles using AFM technique. Surfaces were cleaned and after dip coating in 0.0025 wt.% protein solution in $H_2O$ were dip coated in dispersions of particles at 0.000075, 0.00037 and 0.00075 wt.% for 1, 180, 600, 1800, 3600 and 5400 s. AFM measurements for each concentration at each deposition time were performed multiple times and so that a number of independent regions of the surface were scanned for each sample. AFM measurements of particles with different sizes showed that particles on their own are removed when the surface is rinsed with water (see Fig. 5a). Fig. 5b shows an exam-

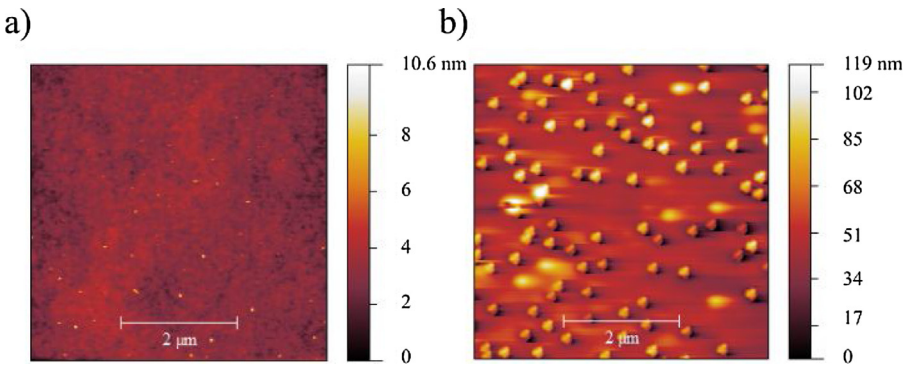


**Fig. 5.** AFM image of a 25 μm$^2$ area of the substrate (a) after rinsing with the large (PS3) particles with no pre-adsorbed layer of proteins and (b) with a pre-adsorbed layer of proteins. *Moringa* protein solution was 0.0025 wt.% concentration and the particles were dispersed at 0.0075 wt.% for these samples. Note the vertical scale is different in the two images as the surface without protein, and consequently without bound particles, shows few topographic features.

ple of an AFM image of the surface after rinsing with a dispersion with 0.00075 wt.% of the large (PS3) particles from the surface that had a pre-adsorbed layer of *Moringa* protein. It is evident from a comparison of Fig. 5a and b that the protein layer causes the particles to stick to the surface. The freely available Matlab function, *CircleFinder* [42], was used to count the number of particles on each image.

For a suspension with a concentration φ in wt.%, the number of particles per unit volume, $N_V$ is:

$$N_V = 0.01\varphi\rho_m/m_p \quad (5)$$

where $\rho_m$ is the density of the particles and $m_p$ is the average mass of a particle. The number of particles, $N_A$, sticking to a planar substrate is given by [43,44]:

$$N_A = pN_V\sqrt{(0.5D_c t)} \quad (6)$$

where $t$ is the exposure time, p is the sticking probability for a particle that collides with the surface, and $D_c$ the diffusion coefficient of the colloidal particle. The diffusion coefficient is given by the Einstein relation as:

$$D_c = k_B T/(6\pi\eta r) \quad (7)$$

with η the viscosity of the medium, $r$ the radius of the particle, $k_B$ the Boltzmann constant and $T$ the absolute temperature. The experimental sticking probability can be estimated from the gradient, α, of a plot of the number of particles per unit area against $t^{1/2}$.

$$p = \alpha/[N_A\sqrt{(0.5D_c)}] \quad (8)$$

The deposition rate of the particles (number of particles attached to the surface per unit area) versus the square root of exposure time at different particles concentrations is shown in Fig. 6. Data points presented in Fig. 6 are the average values of coverage from 9 different areas for each sample exposure time. The sticking probability of the particles from this method was found to be approximately 1 which suggests that particles that hit the surface, adhere irreversibly. However, in the absence of a protein layer, no particles were found on the rinsed surface (Fig. 5a), corresponding to sticking probability of 0. This indicates that the adsorbed protein can act as a 'glue' to bind the particles to the surface.

Despite the fact that AFM provides a reasonable estimate of sticking probabilities, the method still suffers from some limitations. For example, it is only possible to investigate sticking probability at low concentration of particles because in higher concentrations, the formation of multilayers of particles does not allow us to easily count the number of particles. In higher concentrations, similar charge repulsion force between particles may affect the sticking probability and surface coverage [43]. In addition to multilayer formation, the type of AFM technique used in this study

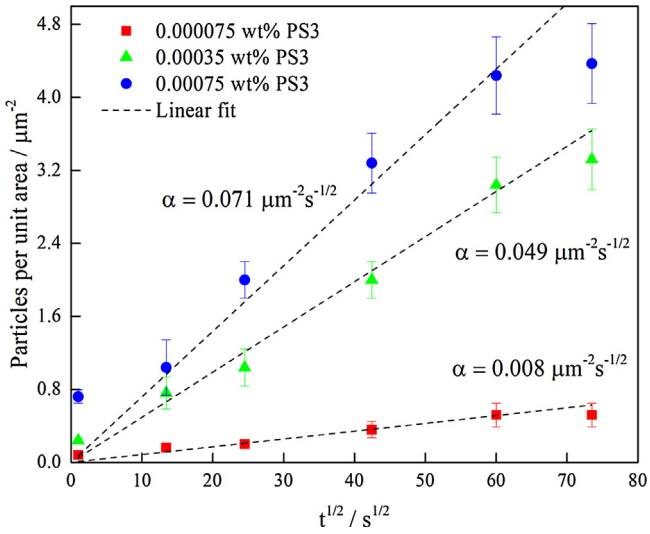


**Fig. 6.** The number of particles stuck to the surface per unit area for three different concentrations of the dispersion of large (PS3) at different deposition times. The dashed line fits are constrained to go through the origin.

requires dried samples. Capillary forces generated by the menisci as the liquid film evaporates are believed to pull the particles together and change the structure of particles [45]. If particles were irreversibly locked on the surface with no mobility, the structure would remain unchanged. Further studies using in-situ measurements such as neutron scattering can provide complementary quantitative information.

## 4. Summary of conclusions and outlook

New experimental results have shown that *Moringa oleifera* seed proteins can be used as a 'glue' for negatively charged latex particles at the silica/water interface. Counting particles that adhered from dilute dispersions indicated a sticking probability of about 1. Further, particles once attached could not be removed by rinsing with either water or a solution of the cationic surfactant $C_{16}$TAB.

Neutron reflection experiments indicated that simple exposure of latex particles to a pre-adsorbed layer of protein at the silica interface gave rise to an average coverage of small particles, radius 350 Å, of 17 % and of large particles, 720 Å, of 13 %. However, the results from AFM and neutron reflection indicate show that the layers are not uniform. In some areas, compact regions of particles are formed while there are fewer particles on parts of the surface. It is possible that capillary forces that occur during drying are sufficient to induce some lateral mobility of the bound particles. The

AFM image of a sample after neutron experiments indicated that there were areas of the interface with highly ordered coverage of particles.

The results, in combination with the knowledge from prior studies, offer several interesting prospects. For example, it has been observed previously [14] that protein can be removed from an alumina surface with $C_{16}$TAB. This suggests that it might be possible to develop surfaces that would release particular types of particles or to use surfaces that have been patterned with different materials to control the adherence and create specific structures on those patterns. Future studies on binding of particles and release would be interesting. Further experiments are also desirable to investigate how the structure alters with different particle concentrations and how it changes with time. The present QCM-D experiments have indicated that repeated cycles of adding protein solution, rinsing and adding more particles can increase the mass at the interface. This process would need further development and testing to establish whether uniform multilayers can be achieved over large areas.

## Acknowledgments

The work was supported in part by the Swedish Research Council (grants 348-2011-7241 and 621-2012-4382) and we thank the ISIS Facility, Chilton, Oxfordshire, U.K (RB 1510461) for the allocation of measurement time and raw data are published [46]. We also thank the Ångström Laboratory workshop for making the sample holders.

## Appendix A. Supplementary data

Supplementary data associated with this article can be found, in the online version, at https://doi.org/10.1016/j.colsurfb.2018.01.004.

## References

[1] B. Verdcourt, A synopsis of the moringaceae, Kew Bull. 40 (1985) 1–23, http://dx.doi.org/10.2307/4108470.
[2] M.E. Olson, J.W. Fahey, Moringa oleifera: un árbol multiusos para las zonas tropicales secas Moringa oleifera: a multipurpose tree for the dry tropics, Revista Mexicana de Biodiversidad 82 (2011) 1071–1082.
[3] J. Shindano, C. Kasase, Moringa (Moringa oleifera): a source of food and nutrition, medicine and industrial products, ACS Symposium Series [0097-6156] 1021 (2009) 421–467, http://dx.doi.org/10.1021/bk-2009-1021.ch024.
[4] U. Eilert, B. Wolters, A. Nahrstedt, The antibiotic principle of Moringa oleifera and Moringa stenopetala, Planta Med. 42 (1981) 55–61, http://dx.doi.org/10.1055/s-2007-971546.
[5] H. Barth, M. Habs, R. Klute, S. Mueller, B. Tauscher, Trinkwasseraufbereitung mit Samen von Moringa oleifera (Lam.), Chemiker Zeitung 16 (1982) 75–78.
[6] M. Madsen, J. Schlundt, E.F. Omer, Effect of water coagulation by seeds of Moringa oleifera on bacterial concentrations, J. Trop. Med. Hyg. 90 (1987) 101–109.
[7] S.K. Kansal, A. Kumari, Potential of M. oleifera for the treatment of water and wastewater, Chem. Rev. 114 (2014) 4993–5010, http://dx.doi.org/10.1021/cr400093w.
[8] J. Gregory, S. Barany, Adsorption and flocculation by polymers and polymer mixtures, Adv. Colloid Interf. Sci. 169 (2011) 1–12, http://dx.doi.org/10.1016/j.cis.2011.06.004.
[9] R. Maikokera, H.M. Kwaambwa, Interfacial properties and fluorescence of a coagulating protein extracted from Moringa oleifera seeds and its interaction with sodium dodecyl sulphate, Colloids Surf. B: Biointerfaces 55 (2007) 173–178, http://dx.doi.org/10.1016/j.colsurfb.2006.11.029.
[10] H.M. Kwaambwa, R. Maikokera, Air-water interface interaction of anionic, cationic, and nonionic surfactants with a coagulant protein extracted from Moringa oleifera seeds studied using surface tension probe, Water SA 33 (2007) 583–588.
[11] H.M. Kwaambwa, M. Hellsing, A.R. Rennie, Adsorption of a water treatment protein from Moringa oleifera seeds to a silicon oxide surface studied by neutron reflection, Langmuir 26 (2010) 3902–3910, http://dx.doi.org/10.1021/la9031046.
[12] H.M. Kwaambwa, A.R. Rennie, Interactions of surfactants with a water treatment protein from moringa oleifera seeds in solution studied by zeta-potential and light scattering measurements, Biopolymers 97 (2012) 209–218, http://dx.doi.org/10.1002/bip.22014.
[13] M.S. Hellsing, H.M. Kwaambwa, F.M. Nermark, B.B.M. Nkoane, A.J. Jackson, M.J. Wasbrough, I. Berts, L. Porcar, A.R. Rennie, Structure of flocs of latex particles formed by addition of protein from Moringa seeds, Colloids Surf. A: Physicochem. Eng. Aspects 460 (2014) 460–467, http://dx.doi.org/10.1016/j.colsurfa.2013.11.038.
[14] H.M. Kwaambwa, M.S. Hellsing, A.R. Rennie, R. Barker, Interaction of Moringa oleifera seed protein with a mineral surface and the influence of surfactants, J. Colloid Interf. Sci. 448 (2015) 339–346, http://dx.doi.org/10.1016/j.jcis.2015.02.033.
[15] A. Ullah, R. Barros Mariutti, R. Masood, I.P. Caruso, G.H. Gravatim Costa, C.M. de Freita, C. Ramos Santos, L.M. Zanphorlin, M.J. Rossini Mutton, M.T. Murakami, R.K. Arni, Crystal structure of mature 2S albumin from Moringa oleifera seeds, Biochem. Biophys. Res. Comm. 468 (2015) 365–371, http://dx.doi.org/10.1016/j.bbrc.2015.10.087.
[16] M. Moulin, E. Mossou, L. Signor, S. Kieffer-Jaquinod, H. M. Kwaambwa, F. Nermark, Y. Caspar, P. Gutfreund, E. P. Mitchell, M. Haertlein, V. T. Forsyth, A. R. Rennie, (2018), Submitted manuscript.
[17] H.A. Jerri, K.J. Adolfsen, L.R. McCullough, D. Velegol, S.B. Velegol, Antimicrobial sand via adsorption of cationic moringa oleifera protein, Langmuir 28 (2012) 2262–2268, http://dx.doi.org/10.1021/la2038262.
[18] K. Shebek, A.B. Schantz, I. Sines, K. Lauser, S. Velegol, M. Kumar, The flocculating cationic polypetide from moringa oleifera seeds damages bacterial cell membranes by causing membrane fusion, Langmuir 31 (2015) 4496–4502, http://dx.doi.org/10.1021/acs.langmuir.5b00015.
[19] J.E.C. Freire, I.M. Vasconcelos, F.B.M.B. Moreno, A.B. Batista, M.D.P. Lobo, M.L. Pereira, J.P.M.S. Lima, R.V.M. Almeida, A.J.S. Sousa, A.C.O. Monteiro-Moreira, J.T.A. Oliveira, T.B. Grangeiro, Mo-CBP3, an antifungal chitin-binding protein from Moringa oleifera seeds, is a member of the 2S albumin family, PLoS One 10 (2015) 1–24, http://dx.doi.org/10.1371/journal.pone.0119871.
[20] B.A. Nordmark, T.M. Przybycien, R.D. Tilton, Comparative coagulation performance study of Moringa oleifera cationic protein fractions with varying water hardness, J. Environ. Chem. Eng. 4 (2016) 4690–4698, http://dx.doi.org/10.1016/j.jece.2016.10.029.
[21] M.S. Hellsing, V. Kapaklis, A.R. Rennie, A.V. Hughes, L. Porcar, Crystalline order of polymer nanoparticles over large areas at solid/liquid interfaces, Appl. Phys. Lett. 100 (2012) 221601, http://dx.doi.org/10.1063/1.4723634.
[22] A. Kosiorek, W. Kandulski, P. Chudzinski, K. Kempa, M. Giersig, Shadow nanosphere lithography: simulation and experiment, Nano Lett. 4 (2004) 1359–1363, http://dx.doi.org/10.1021/nl049361t.
[23] H.-J. Butt, B. Cappella, M. Kappl, Force measurements with the atomic force microscope: technique, interpretation and applications, Surf. Sci. Rep. 59 (2005) 1–152, http://dx.doi.org/10.1016/j.surfrep.2005.08.003.
[24] E. Servoli, D. Maniglio, M.R. Aguilar, A. Motta, J. San Roman, L.A. Belfiore, C. Migliaresi, Quantitative analysis of protein adsorption via atomic force microscopy and surface plasmon resonance, Macromol. Biosci. 8 (2008) 1126–1134, http://dx.doi.org/10.1002/mabi.200800110.
[25] L.E. Averett, M.H. Schoenfisch, Atomic force microscope studies of fibrinogen adsorption, Analyst 135 (2010) 1201–1209, http://dx.doi.org/10.1039/B924814E.
[26] G. Sauerbrey, Verwendung von Schwingquarzen zur Wägung dünner Schichten und zur Mikrowägung, Zeit. f. Physik 155 (1959) 206–222, http://dx.doi.org/10.1007/BF01337937.
[27] M. Rodahl, F. Höök, A. Krozer, P. Brzezinski, B. Kasemo, Quartz crystal microbalance setup for frequency and Q-factor measurements in gaseous and liquid environments, Rev. Sci. Inst. 66 (1995) 3924–3930, http://dx.doi.org/10.1063/1.1145396.
[28] I. Reviakine, D. Johannsmann, R.P. Richter, Hearing what you cannot see and visualizing what you hear: interpreting quartz crystal microbalance data from solvated interfaces, Anal. Chem. 83 (2011) 8838–8848, http://dx.doi.org/10.1021/ac201778h.
[29] E. Tellechea, D. Johannsmann, N.F. Steinmetz, R.P. Richter, I. Reviakine, Model-independent analysis of QCM data on colloidal particle adsorption, Langmuir 25 (2009) 5177–5184, http://dx.doi.org/10.1021/la803912p.
[30] J. Webster, S. Holt, R. Dalgliesh, INTER the chemical interfaces reflectometer on target station 2 at ISIS, Physica B 385–386 (2006) 1164–1166, http://dx.doi.org/10.1016/j.physb.2006.05.400.
[31] A.R. Rennie, M.S. Hellsing, E. Lindholm, A. Olsson, Note: sample cells to investigate solid/liquid interfaces with neutrons, Rev. Sci. Inst 86 (2015) 016115, http://dx.doi.org/10.1063/1.4906518.
[32] R. Maikokera, Physicochemical and Conformational Studies of a Water Treatment Coagulant Protein Extracted from Moringa Oleifera Seeds. Ph.D. Thesis, Chemistry, University of Botswana, 2008.
[33] V.F. Sears, Neutron scattering lengths and cross sections, Neutron News 3 (3) (1992) 26–37, http://dx.doi.org/10.1080/10448639208218770.
[34] A. R. Rennie, (2017). http://www.reflectometry.net/reflect.htm#Analysis.
[35] M.S. Hellsing, A.R. Rennie, R.K. Heenan, S.E. Rogers, Structure of a large colloidal crystal –controlling orientation and three-dimensional order, RSC Adv. 2 (2012) 7091–7098, http://dx.doi.org/10.1039/C2RA21092D.
[36] A.R. Rennie, M.S. Hellsing, K. Wood, E.P. Gilbert, L. Porcar, R. Schweins, C.D. Dewhurst, P. Lindner, R.K. Heenan, S.E. Rogers, P.D. Butler, J.R. Krzywon, R.E. Ghosh, A.J. Jackson, M. Malfois, Learning about SANS instruments and data reduction from round robin measurements on samples of polystyrene latex, J. Appl. Crystallogr. 46 (2013) 1289–1297, http://dx.doi.org/10.1107/S0021889813019468.

[37] S. Nouhi, M.S. Hellsing, V. Kapaklis, A.R. Rennie, Grazing incidence small angle neutron scattering from structures below an interface, J. Appl. Cryst. 50 (2017) 1066–1074, http://dx.doi.org/10.1107/S1600576717007518.
[38] Biolin Scientific, 2017 http://www.biolinscientific.com/qsense/qsensors.
[39] M.V. Voinova, M. Rodahl, M. Jonson, B. Kasemo, Viscoelastic acoustic response of layered polymer films at fluid-solid interfaces: continuum mechanics approach, Phys. Scr. 59 (1999) 391–396, http://dx.doi.org/10.1238/Physica.Regular.059a00391.
[40] M. S. Hellsing, F. Höök (2018) manuscript in preparation.
[41] Y. Yoneda, Anomalous surface reflection of X rays, Phys. Rev. 131 (1963) 2010–2013, http://dx.doi.org/10.1103/PhysRev.131.2010.
[42] B. Shoelson, Circle Finder, 2016 https://se.mathworks.com/matlabcentral/fileexchange/34365-circle-finder.
[43] C.A. Johnson, A.M. Lenhoff, Adsorption of charged latex particles on mica studied by atomic force microscopy, J. Colloid Interf. Sci. 179 (1996) 587–599, http://dx.doi.org/10.1006/jcis.1996.0253.
[44] C.D. Keating, M.D. Musick, M.H. Keefe, M.J. Natan, Kinetics and thermodynamics of Au colloid monolayer self-assembly, J. Chem. Educ. 76 (1999) 949–955, http://dx.doi.org/10.1021/ed076p949.
[45] K.D. Danov, B. Pouligny, P.A. Kralchevsky, Capillary forces between colloidal particles confined in a liquid film: the finite-Meniscus problem, Langmuir 17 (2001) 6599–6609, http://dx.doi.org/10.1021/la0107300.
[46] A.R. Rennie, S. Nouhi, M.S. Hellsing, H.M. Kwaambwa, M. Skoda, Binding Particles with Proteins at Interfaces, 2015, pp. 1510461, http://dx.doi.org/10.5286/ISIS.E.61784148 (STFC ISIS Facility).